Interuser interference in adjacent wireless body area networks

Wu, Xianyue; Nechayev, Yuriy; Constantinou, Constantinos; Hall, Peter

DOI:
10.1109/TAP.2015.2465856

Document Version
Publisher's PDF, also known as Version of record

Citation for published version (Harvard):
Wu, X, Nechayev, Y, Constantinou, C & Hall, P 2015, 'Interuser interference in adjacent wireless body area networks', *IEEE Transactions on Antennas and Propagation*, vol. 63, no. 10, pp. 4496-4504. https://doi.org/10.1109/TAP.2015.2465856

Inter-user Interference in Adjacent Wireless Body Area Networks

Xianyue Wu, *Member, IEEE,* Yuriy I. Nechayev, *Member, IEEE,* Costas C. Constantinou, *Member, IEEE,* and Peter S. Hall, *Fellow, IEEE*

***Abstract*—The inter-user interference between wireless body area networks worn by two moving persons in an indoor environment at 60 GHz and 2.45 GHz is investigated experimentally. Both omni-directional antennas (monopoles) and directional antennas (horns) were used in the measurements. The interference power level variation and carrier-to-interference ratio were measured and characterized. Median interference power level reduction of nearly 20 dB was achieved in all measured channels by adopting 60 GHz radio transmissions compared to 2.45 GHz, both with omni-directional on-body antennas. A further 20 dB of interference level reduction was achieved at 60 GHz by adopting directional antennas confining the radiated wave along the body surface. Level crossing rates for interference power variation using omni-directional antennas range from 2.7–7.2 s^{-1} at 2.45 GHz and 32–64 s^{-1} at 60 GHz for static to progressively more dynamic links, whereas the corresponding range using 60 GHz directional antennas is reduced to 39–54 s^{-1}. The median improvement in the instantaneous carrier-to-interference ratio for the chest-head channel between 60 GHz and 2.45 GHz was approximately 30 dB. The measured interference power level and carrier-to-interference ratio, in dB, were found to satisfactorily fit the normal distribution according to the normalized root mean square error based fit metric.**

Wireless body area network, interference, 60 GHz, carrier-to-interference ratio, body movements.

I. Introduction

The advent of wireless body area networks (WBANs) and their use in a wide range of applications, from consumer electronics to military purposes, dictates the need to investigate in depth the behavior of antennas and wave propagation around the human body. Although this area has been extensively studied in the past decade [1], certain issues remain unresolved for communication systems based on WBANs at the industrial, scientific and medical (ISM) and ultra-wideband (UWB) bands. Such issues include compact and highly efficient antenna design, privacy and security, interference mitigation and achieving high data rates above one gigabit per second. The interference issue is a vital consideration in WBAN design. It is expected that the operation of multiple WBANs will not be coordinated, as these will be fully autonomous. Hence, a WBAN may cause severe interference to a second co-channel WBAN when in close proximity, especially in densely populated environments such as shopping malls, hospital wards, etc. This event is referred to as a "network collision" [2]. Previous research shows that the impact of inter-user interference is significant and needs to be addressed if WBANs are to be extensively and successfully deployed [3]. The nature of human movements means the network collisions may be either transient, e.g. people passing by each other in the street, or be of very long duration, e.g. patients co-located in the same ward in hospital for many hours. The cellular approach for interference mitigation [4] is not applicable to WBANs because of their mobile and variable nature.

The interference issue has been addressed for WBANs operating below 10 GHz and several solutions for this problem have been proposed. These include using a fixed sensor network to monitor indoor wireless body sensor networks (WBSNs) and sending a request to these WBSNs to alter the operation of their protocols [3], employing power control, and using interference cancelation with an interrupted transmission scheme [5]. Since a low power spectral density of less than -41.3 dBm/MHz is mandated for UWB communications, UWB systems will not cause significant interference to existing narrowband systems. However, the UWB signal is vulnerable to narrowband interference (NBI) from existing high-power narrowband wireless systems. Some NBI suppression techniques have been proposed, such as adaptive notch filters and optimal pre/post-rake UWB transceivers [6], [7], but these methods significantly increase system complexity.

Many studies on inter-body channel characterization have been reported [8]–[12], but the research on interference for WBANs at the physical layer is relatively limited. Although the interference issue is usually handled at the Medium Access Control (MAC) layer or at higher protocol layers of the communication architecture, it needs to be quantified and hence understood at the physical layer. The measurement of interference for WBANs at 2.45 GHz has been reported in [13], [14], but only static postures were considered in these studies. The dynamics of the human body posture and movement are the dominant determiners of on-body link performance, as well as WBAN-WBAN interference links. Hence, body movements should be taken into account in WBAN channel characterization. In addition, to the best of the authors' knowledge, the only work related to 60 GHz WBAN-WBAN interference was conducted in [15]. In this work, ray-tracing simulations were performed to calculate the signal coverage in an indoor environment at both 2.45 GHz and 60 GHz. The antennas used in the simulation were isotropic antennas. Results show that the use of 60 GHz WBANs achieves about 20 dB higher carrier-to-interference ratio (CIR) compared to 2.45 GHz WBANs. However, [15] does not

X. Wu and Y.I. Nechayev were with the University of Birmingham, Edgbaston, Birmingham, B15 2TT, UK. They are now with Huawei, Shanghai, and Moscow, respectively (e-mail: Xianyue.Wu.Mr@ieee.org).

C.C. Constantinou and P.S. Hall are with the University of Birmingham, Edgbaston, Birmingham, B15 2TT, UK (e-mail: c.constantinou@bham.ac.uk).

This article has been accepted for publication in a future issue of this journal, but has not been fully edited. Content may change prior to final publication. Citation information: DOI 10.1109/TAP.2015.2465856, IEEE Transactions on Antennas and Propagation

include body movements. It is expected that the CIR can be improved further by employing directional antennas at 60 GHz. Based on this study, a recent alternative wireless solution for body area networks is to adopt the 60 GHz radio band [16]. The adoption of the 60 GHz band has significant advantages for WBANs: Specifically, these are the very small size of body-mounted equipment, high signal integrity and low visibility at the RF level due to good radiation control using directional or reconfigurable antennas, high attenuation beyond the body area and easily achievable data rates of several gigabits per second. Initial research has been carried out quantifying the characteristics of 60 GHz body area networks, including wearable antenna design [17]–[20], on-body channel characterization [21], [22] and preliminary interference and covertness studies [23], [24].

This paper investigates the inter-user interference between WBANs on two persons undertaking a variety of body movements in an indoor environment at 60 GHz and 2.45 GHz. The paper is organized as follows: In Section II, the measurement procedures for interference power variation and CIR are described. Measured results of interference power variation and CIR are presented and discussed in Section IV. Conclusions are drawn in Section V.

II. Measurement Procedures

A. Interference power variation measurements

Interference power variation measurements were performed in a laboratory in the Electronic, Electrical and Systems Engineering building at the University of Birmingham. For each measurement, two identical antennas were placed on the bodies of two men of height 1.65 m and 1.83 m, respectively. Antenna placements on the body were chosen to represent the topology of a WBAN which consists of a number of wearable devices positioned at different locations on the human body, including the abdomen (e.g. mobile phone, or other body area data aggregator), head (e.g. headphones, head-mounted display), wrist (e.g. smart watch, physiological sensor), and chest (e.g. electrocardiography sensor, repeater nodes necessary to establish longer mm-wave links), as shown in Fig. 1. The symmetry in the placement of the antennas is arbitrary, but of little practical consequence due to the random relative motion of the two persons. The intention was to have a variety of node positions with highly exposed antennas to the surrounding environment (e.g. on the head), highly mobile antennas (e.g. on the wrist) and more static, less exposed antennas (e.g. on the abdomen or chest). Therefore, six interference channels were investigated, namely the abdomen-abdomen, head-abdomen, head-head, head-wrist, wrist-abdomen, and wrist-wrist links. Only one interference channel was measured at any one time.

Antennas used in these measurements were rectangular ground-plane monopole antennas at 2.45 GHz, a circular ground-plane monopole antenna at 60 GHz and standard gain pyramidal horn antennas at 60 GHz. Fig. 2 shows a 2.45 GHz monopole antenna (4 dBi gain, 42° E-plane 3-dB beamwidth in free-space) placed on the wrist of human body. The ground plane of this antenna is 80 mm × 80 mm. The separation between the antenna and the body surface was 20 mm. Fig. 3

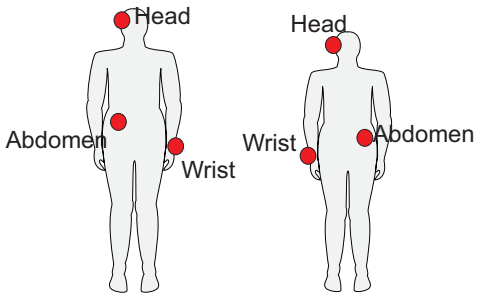

Fig. 1. Antenna placements on the human body.

shows various placements of a 60 GHz monopole antenna (4.8 dBi gain, 34° E-plane 3-dB beamwidth in free-space) on the human body. This antenna is made from a 60 GHz semi-rigid coaxial cable with a protruding center conductor soldered onto a copper disk ground plane. The ground plane diameter is 25 mm and its height above the skin was approximately 13 mm. The insertion loss of the short feed cable of the monopoles was less than 0.5 dB. Monopoles have a near omni-directional pattern in the azimuth plane tangential to the body surface (H-plane), which renders the results independent of the antenna orientation. The horn antennas were Flann© standard gain horns Series 240 model 25240 (20 dBi gain, 20° 3-dB beamwidth in both the E- and H-planes in free space). When a horn antenna was placed on the wrist and abdomen, the aperture of the antenna was facing upwards. When a horn antenna was placed on the head, the aperture of the antenna was facing downwards, as shown in Fig. 4.

Figs. 5 and 6 show the simulated radiation pattern of the 60 GHz horn and 60 GHz monopole antennas described above, in close proximity to a skin phantom ($90\times60\times5\mathrm{mm}^3$, complex permittivity = $7.98-j10.9$ at 60 GHz [25]). Both antennas had their polarization normal to the phantom surface. The edge of the horn aperture touched the skin phantom in the simulation model and the distance between the monopole ground plane and the phantom was 1 mm. The simulated realized gains of the horn and monopole antennas in the presence of the skin phantom were 18.7 dBi and 4.9 dBi, respectively. Naturally, the antenna radiation properties were affected by the presence of the phantom, especially for the horn antenna, since its radiating aperture is not shielded by the presence of a ground plane. For monopole antennas, the radiation pattern distortion by the presence of phantom was much less severe. Previous studies [17]–[20] show that the presence of the body has only a slight effect on the impedance match for 60 GHz antennas. At 2.45 GHz, the proximity of the body causes a slight frequency shift in its resonant frequency, but this is still within the operating bandwidth of the antenna.

In order to improve the dynamic range at 60 GHz, two amplifiers were used during the measurements, namely a power amplifier (Spacek Labs Inc.© SP604-13-12W) and a low noise amplifier (Spacek Labs Inc.© SL6010-15-6). The gains of the power amplifier and the low noise amplifier are 23 dB and 16 dB at 60 GHz, respectively.

During the measurements, two subjects performed random

This article has been accepted for publication in a future issue of this journal, but has not been fully edited. Content may change prior to final publication. Citation information: DOI 10.1109/TAP.2015.2465856, IEEE Transactions on Antennas and Propagation

Fig. 2. Monopole antenna on the wrist (2.45 GHz).

(a) (b) (c)

Fig. 3. Placements of monopole antenna with amplifier on the body (60 GHz): (a) Head, (b) Wrist, (c) Abdomen.

(a) (b) (c)

Fig. 4. Placements of horn antenna with amplifier on the body (60 GHz): (a) Head, (b) Wrist, (c) Abdomen.

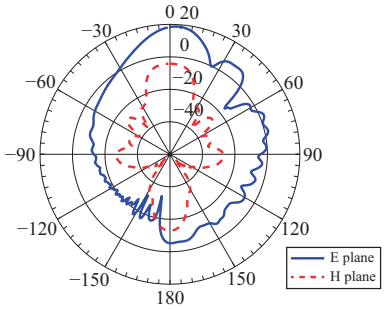

Fig. 5. Simulated radiation pattern for horn antenna on the skin phantom at 60 GHz; boreside is at 0°.

movements and rotations within a 1 m × 2.5 m area in a lab environment as shown in Fig. 7. The room contained equipment, tables, chairs and computers, thus providing a rich multipath propagation environment. The random body movements included walking, waving arms, rotating trunks, squatting, bending trunks, running, etc. The interference in this scenario was expected to be more severe than in daily situations because of the close distance between the two human subjects. The received signal power during the various

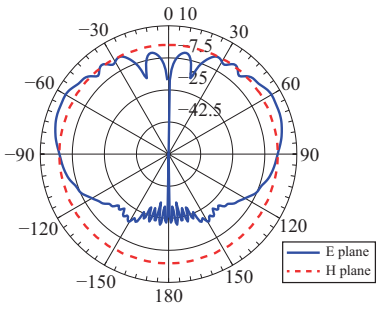

Fig. 6. Simulated radiation pattern for monopole antenna on the skin phantom at 60 GHz.

activities was measured with a Rohde & Schwarz© ZVA 67 Vector Network Analyzer (VNA). The source and receiver direct access ports on the ZVA 67 were used, thus bypassing the directional couplers in order to maximize the dynamic range of the measurements. For the 60 GHz measurement setup, the VNA was set to 60 GHz continuous wave (CW) with 60001 sweep points taken over a sweep time of 62.1 s (i.e. the channel was sampled at 966.2 samples/s in the frequency domain). The output power and intermediate frequency (IF) filter bandwidth were set to 0 dBm and 1 kHz respectively. Two 2 m long cables connected the antennas to the VNA. The insertion loss of these cables was measured and found to be approximately 15 dB as the cables were flexed randomly. It was found that stress caused by rapid movements led to deterioration of the cable performance, as the loss in the cable increased by 1.5 dB after the measurements. A back-to-back calibration was performed before the measurements to normalize the measured signal, and the amplifier gains were removed in the data post-processing. With such a setup, the root mean square (RMS) noise level corresponds to a normalized path loss of -110 dB. For the 2.45 GHz measurement, the VNA settings were the same as the 60 GHz measurements. The RMS noise level at 2.45 GHz is -97 dB after the back-to-back calibration. The loss variation in the cable due to movements were found to be negligible at 2.45 GHz.

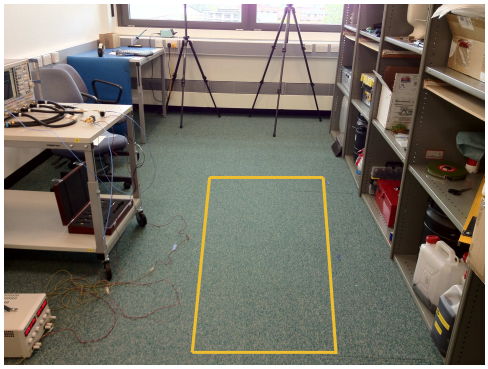

Fig. 7. Lab environment.

B. CIR measurements

The CIR measurements were conducted in the same environment with the same VNA settings as in II-A, except that

This article has been accepted for publication in a future issue of this journal, but has not been fully edited. Content may change prior to final publication. Citation information: DOI 10.1109/TAP.2015.2465856, IEEE Transactions on Antennas and Propagation

the output power was set to 10 dBm. The same two human subjects were involved in this measurement as described previously. One monopole antenna and one horn antenna were placed on each subject for the 60 GHz measurements. Only one antenna was transmitting at any time, whilst the other three antennas were receiving. Hence, there were three channels measured simultaneously. Due to channel reciprocity, these measured channels are equivalent to a scenario with one receiver, one transmitter and two further transmitters acting as interferers. The reason for adopting this measurement method is the limited number of power amplifiers available to support the measurements. The channel on Subject 1 is defined as the wanted-signal channel. The other two channels between the two subjects are defined as the interference channels. Two body channels were measured: the head-abdomen channel and the head-chest channel. We define the following notation to compactly label the antenna type and placement:

$$D^n_{P_D,T_D}, S^m_{P_S,T_S} \tag{1}$$

$$P_D, P_S \in \{Head, Abdomen, Chest\} \tag{2}$$

$$T_D, T_S \in \{H, M\}, m, n \in \{1, 2\} \tag{3}$$

where D, S stand for the destination and source of the link, respectively; P_D and P_S represent the antenna position for the source and destination of the link, respectively; T_D, T_S represent the antenna type. Abbreviations are used to represent antenna type: H for horns and M for monopoles. m and n label the m$^{\text{th}}$ and n$^{\text{th}}$ subjects, respectively. If $m = n$, it means that this channel is the wanted signal; otherwise, it is an interference signal.

The four measured CIR scenarios are listed in Table I. Every scenario corresponds to two CIRs: Scenarios A and B were for the head-abdomen channel and scenarios C and D were for the head-chest channel. Figure 8 illustrates the CIR measurement scenario for head-chest channels. The wrist position was not considered for the CIR measurement because the wanted signal channel terminating on the wrist is very weak.

TABLE I
CIR MEASUREMENTS

Scenario	Signal channel	Interference channel	CIR no.
A	$D^1_{Head,H}$, $S^1_{Abdomen,M}$	$D^1_{Head,H}, S^2_{Head,H}$	(1)
		$D^1_{Head,H}, S^2_{Abdomen,M}$	(2)
B	$D^1_{Abdomen,M}$, $S^1_{Head,H}$	$D^1_{Abdomen,M}, S^2_{Abdomen,M}$	(3)
		$D^1_{Abdomen,M}, S^2_{Head,H}$	(4)
C	$D^1_{Head,H}$, $S^1_{Chest,M}$	$D^1_{Head,H}, S^2_{Head,H}$	(5)
		$D^1_{Head,H}, S^2_{Chest,M}$	(6)
D	$D^1_{Chest,M}$, $S^1_{Head,H}$	$D^1_{Chest,M}, S^2_{Chest,M}$	(7)
		$D^1_{Chest,M}, S^2_{Head,H}$	(8)

An identical back-to-back calibration to the one described in II-A was performed to normalize the measured data for all four ports. The cable movements were characterized and found to result in a maximum fluctuation in the received signal of 1 dB. During the measurements, the two subjects were performing random movements within the fixed area, as described previously. For the 2.45 GHz measurements, four monopole antennas were used with two on each subject. All remaining settings were identical to those used at 60 GHz, except that no amplifiers are employed at 2.45 GHz.

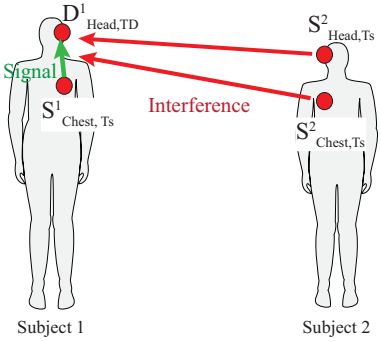

Fig. 8. CIR measurement scenario for head-chest channels.

III. Channel Model

The radio channels in the proposed scenario can be modeled as follows,

$$P_r = P_s \cdot |h_s|^2 + P_i \cdot |h_i|^2 + P_N \tag{4}$$

where P_r is the received power at the receiver, h_s is the channel transfer function for the wanted signal channel measured at the antenna terminals, P_s is the transmit power from the wanted transmitter, P_i is the transmit power of the interferer, h_i is the interference channel transfer function measured at the antenna terminals, and P_N is the power of noise. We assume that the only noise contribution is from the VNA itself and its effect on measured data is removed in the data post-processing through thresholding. Therefore, the CIR can be defined as,

$$\text{CIR} = \frac{P_s \cdot |h_s|^2}{P_i \cdot |h_i|^2} \tag{5}$$

For simplicity in the following sections, we assume that $P_s = P_i$ in all the scenarios studied, simplifying the above equation to CIR $= |h_s|^2/|h_i|^2$. Moreover, the normalized received interference power is $P_I = |h_i|^2$, where the normalization assumes that $P_i = 1$W.

IV. Results and Discussion

A. P_I Results

In processing the measurement data, samples of interference power lower than a certain threshold were excluded from the analysis to eliminate the effects of measurement equipment noise on the channel characteristics. The threshold was chosen to be at the level not exceeded by the noise 99% of the time. For the 60 GHz measurements, the normalized P_I threshold was -103 dB. Any sample of interference below this threshold was discarded. Since all the measured data at 2.45 GHz were above the noise threshold, this process was not applied to the 2.45 GHz measurements. The median ($\tilde{X}$), mean ($\bar{X}$) and

This article has been accepted for publication in a future issue of this journal, but has not been fully edited. Content may change prior to final publication. Citation information: DOI 10.1109/TAP.2015.2465856, IEEE Transactions on Antennas and Propagation

standard deviation (σ_X) of a vector X is used for data analysis. X is either P_I or CIR. The definition of standard deviation is,

$$\sigma_X = \sqrt{\frac{1}{n}\sum_{i=1}^{n}(x_i - \bar{X})^2} \tag{6}$$

where

$$\bar{X} = \frac{1}{n}\sum_{i=1}^{n} x_i \tag{7}$$

and n is the number of elements in X. The normal distribution or truncated normal distribution [26] was fitted to the P_I and CIR data. The probability density function (pdf) of the normal distribution is,

$$f(x \mid \bar{X}, \sigma_X) = \frac{1}{\sigma_X\sqrt{2\pi}} e^{-\left(x-\bar{X}\right)^2 / 2\sigma_X^2} \tag{8}$$

where x describes either P_I or CIR, as appropriate.

A fitness metric based on normalized root mean square error (NRMSE) was used to test how well the data approximates the normal distribution. The fitness metric is defined as,

$$\text{fit} = 1 - \frac{\|x_{model} - x\|}{\|x_{model} - \text{mean}(x_{model})\|} \tag{9}$$

where x is either P_I or CIR, x_{model} are P_I or CIR samples from the normal distribution candidate, $\|\cdot\|$ indicates the 2-norm of a vector, and fit is a scalar value. The NRMSE can vary between $-\infty$ (very bad fit) to 1 (perfect fit). A fit value of 0 implies that the data is as good as the mean value of the model — i.e. the model and the data are in agreement *on average*, allowing for deviations due to experimental errors. A fit value close to 0 thus denotes an adequate fit.

Table II shows the statistics of the interference power level. The median is used instead of the mean in the ensuing discussion as it is not subject to inaccuracy arising from the truncation of the distribution due to noise thresholding when signals are weak. The shape of the distribution of the measurements below the threshold can alter the mean value, but as long as the fraction of the measurements below the noise threshold is known, the median value is known precisely. This occurs for a number of the 60 GHz measurements, especially the case for the CIR data shown in Section IV-B. The median interference power level ($\tilde{P}_I$) of 60 GHz monopoles for the abdomen-abdomen interference channel is 17.5 dB lower than that of 2.45 GHz monopoles. The $\tilde{P}_I$ of 60 GHz horns is about 24 dB lower than that of 60 GHz monopoles. These findings confirm the validity of our assertion that the adoption of 60 GHz radio transmission with directional antennas can reduce WBAN-WBAN interference significantly. Moreover, the standard deviation of P_I (σ_{P_I}) indicates slightly larger interference power variation at 60 GHz because the millimeter wave propagation characteristics and narrower beamwidth of directional antennas result in more severe large-scale fading caused by body movements.

Histograms representing the pdfs of the measured P_I for the abdomen-abdomen, wrist-head, wrist-wrist interference channels are shown in Figs. 9, 10 and 11, respectively, where P_I is expressed in dB. The figures show P_I together with the best least-mean-squares-fit normal distribution. The NRMSE fit values of the candidate model are shown in Table III. The apparent poor fit for the distribution of P_I in the case of 60 GHz horn antennas in Fig. 9 is due to the significant truncation of the distribution arising from the severely noise limited measurements, in conjunction with the fact that the normalization of the NRMSE does not measure the absolute deviation between the data and the model. The NRMSE is better than -0.42 and thus the normal distribution represents an adequate fit. The reason for the fit being merely adequate is that the measured probability distributions are often characterized by multiple peaks and exhibit link-specific shape-variability. This is because the measured on-body channel data is known to be non-stationary, and large data sets encompassing very differing human activities are convolved together. These findings agree with previous studies for on-body channels [21], [27]. The

TABLE II
DATA STATISTICS FOR P_I (dB)

Interference channels	Frequency & Antennas	$\tilde{P}_I$	$\bar{P}_I$	σ_{P_I}
Abdomen-Abdomen	2.45 GHz mono	-48.3	-48.8	7.7
	60 GHz mono	-65.7	-65.8	10.2
	60 GHz horn	-89.4	-88.4	9.9
Abdomen-Head	2.45 GHz mono	-50.1	-50.5	7.2
	60 GHz mono	-69.6	-69.5	9.1
	60 GHz horn	-89.4	-88.4	9.4
Head-Head	2.45 GHz mono	-47.3	-47.9	6.7
	60 GHz mono	-67.4	-67.4	9.4
	60 GHz horn	-86.7	-86.6	9.0
Wrist-Abdomen	2.45 GHz mono	-49.3	-49.6	7.7
	60 GHz mono	-69.4	-68.9	9.6
	60 GHz horn	-87.9	-87.3	8.9
Wrist-Head	2.45 GHz mono	-48.6	-49.0	7.4
	60 GHz mono	-67.3	-67.3	8.9
	60 GHz horn	-87.9	-87.6	7.6
Wrist-Wrist	2.45 GHz mono	-48.3	-48.7	7.4
	60 GHz mono	-68.5	-68.4	8.9
	60 GHz horn	-86.9	-86.2	8.8

TABLE III
FIT VALUES FOR PROBABILITY DISTRIBUTION SELECTION OF P_I

Interference channels	Frequency & Antennas	fit(Normal)
Abdomen-Abdomen	2.45 GHz mono	-0.41
	60 GHz mono	-0.41
	60 GHz horn	-0.42
Abdomen-Head	2.45 GHz mono	-0.42
	60 GHz mono	-0.41
	60 GHz horn	-0.42
Head-Head	2.45 GHz mono	-0.41
	60 GHz mono	-0.42
	60 GHz horn	-0.42
Wrist-Abdomen	2.45 GHz mono	-0.42
	60 GHz mono	-0.41
	60 GHz horn	-0.41
Wrist-Head	2.45 GHz mono	-0.42
	60 GHz mono	-0.41
	60 GHz horn	-0.42
Wrist-Wrist	2.45 GHz mono	-0.41
	60 GHz mono	-0.41
	60 GHz horn	-0.42

This article has been accepted for publication in a future issue of this journal, but has not been fully edited. Content may change prior to final publication. Citation information: DOI 10.1109/TAP.2015.2465856, IEEE Transactions on Antennas and Propagation

parameters of the fitted statistical distribution for all the measured data are summarized in Table II.

The main factors contributing to the observed interference level reduction are antenna directivity and carrier frequency. The narrow beamwidth radiation pattern of directional antennas reduces the probability of the main radiation lobe illuminating an interferer significantly. This in turn reduces the mean interference signal compared to omni-directional antennas. The higher radio carrier frequency corresponds to a smaller antenna effective aperture for equal gain antennas (e.g. when comparing monopoles at the two frequency bands), which also results in reduced interference power levels. Antenna location may affect the interference level for some specific channels such as the abdomen-abdomen interference channel where shadowing obstruction may be caused by hand movements, but as can be seen in Table II the antenna location is not a major factor compared to antenna directivity and carrier frequency. However, the random movements of the subjects contribute to the interference power variation especially when employing directional (horn) antennas.

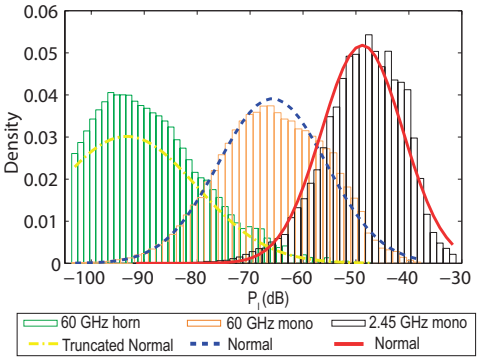

Fig. 9. Distributions of P_I for abdomen-abdomen interference channel.

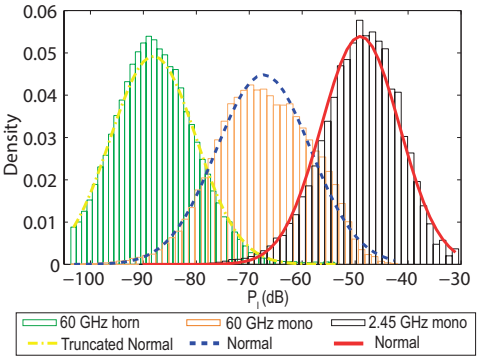

Fig. 10. Distributions of P_I for wrist-head interference channel.

The level-crossing rate (LCR) was also calculated for P_I for all measured channels and is shown in Fig. 12. It is defined as the number of times per second P_I is crossing a certain threshold power level indicated by the abscissa. The LCR is much higher at 60 GHz compared to 2.45 GHz. Maximum level crossing rates for P_I using omni-directional antennas range from 2.7–7.2 s^{-1} at 2.45 GHz and 32–64 s^{-1} at 60 GHz for static to progressively more dynamic links, whereas the

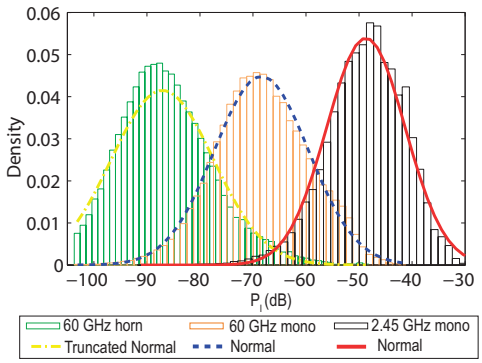

Fig. 11. Distributions of P_I for wrist-wrist interference channel.

corresponding range when using 60 GHz directional antennas is reduced to 39–54 s^{-1}. By comparing the LCR for 60 GHz monopoles and the LCR for 60 GHz horn antennas, it can be seen that the more spatially confined radiation pattern of horn antennas has a significant impact on the LCR. The wrist-to-wrist interference channel exhibits the largest peak LCRs consistently. This is thought to be a consequence of the highly dynamic nature of the received signal arising from the large displacement movements experienced by the antenna positioned on the wrist, which indicates that links terminating on the wrist have a larger probability of being subject to significant interference. The interference channels terminating on the abdomen and head change at a much slower rate in comparison.

B. CIR Results

For the CIR calculation, if either the wanted signal or the interference was found to be below the noise threshold, the data was discarded. The CIR statistics for all measured channels at 60 GHz are listed in Table IV, using the notation introduced earlier to represent the specific CIR channel considered in each case. Every CIR expression has three terms denoting the receiver, the transmitter and the interferer with their respective antenna type and placement. In comparing scenarios C and D, it can be readily observed that the CIR measurement no. (5) achieved the highest $\widetilde{\text{CIR}}$, because both the receiver and interferer were using horn antennas. As discussed in Section IV-A, directional antennas mitigate the interference level significantly. In contrast, the CIR measurement no. (7) gives the lowest $\widetilde{\text{CIR}}$, because the receiver and interferer antennas were both monopoles. The 3.61 dB $\widetilde{\text{CIR}}$ difference between CIR measurements (6) and (8) is thought to have been caused by the inability of the subjects to perform precisely repeatable random movements during the measurements and also because the subjects have different physical characteristics, when the nodes are placed in reversed positions for the two links under investigation. The same conclusion can be reached in comparing scenarios A and B.

One of the major differences between scenarios A and C was the transmitter-receiver separation on Subject 1. A larger than 20 dB $\widetilde{\text{CIR}}$ improvement for the head-chest channel was observed compared to the head-abdomen channel. This is

This article has been accepted for publication in a future issue of this journal, but has not been fully edited. Content may change prior to final publication. Citation information: DOI 10.1109/TAP.2015.2465856, IEEE Transactions on Antennas and Propagation

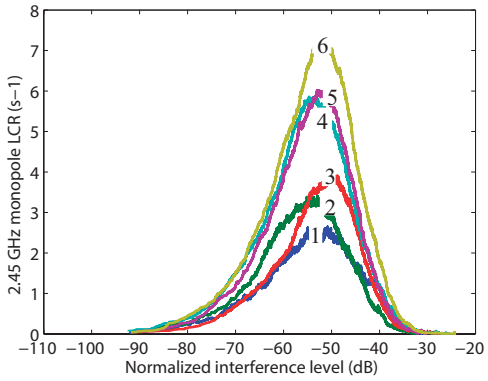

(a)

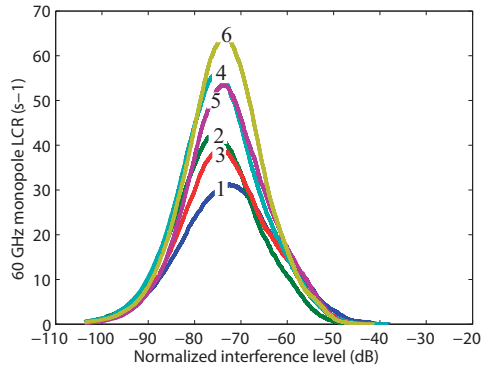

(b)

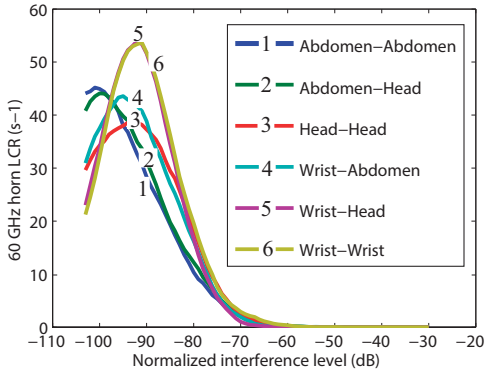

(c)

Fig. 12. LCR for P_I: (a) 2.45 GHz monopoles, (b) 60 GHz monopoles, (c) 60 GHz horns.

probably because of the longer physical link length on Subject 1 (who was taller) and also the obstruction by the hand due to body movements for the head-abdomen channel.

The measured CIRs at 2.45 GHz are listed in Table V, using identical notation to that in Table IV, whilst omitting the antenna type parameter which is always a monopole for brevity. Scenarios A', B', C' and D' are directly comparable to the 60 GHz Scenarios A, B, C and D, respectively. Up to 8.8 dB $\widetilde{\text{CIR}}$ was achieved for the chest-head channel. For the abdomen-head channel, the $\widetilde{\text{CIR}}$ was about 0 dB. This means that the wanted signal can be almost as strong as the interference signal, which is possible when none of the discussed interference reduction techniques in I are applied at 2.45 GHz.

From the head-abdomen channel statistics presented in Tables IV and V, up to 10.4 dB $\widetilde{\text{CIR}}$ improvement over 2.45 GHz can be observed at 60 GHz when the interferer antenna is a monopole; if the interferer antenna is a horn, up to 15.5 dB $\widetilde{\text{CIR}}$ improvement can be achieved. This $\widetilde{\text{CIR}}$ improvement for the head-chest channel, was observed to be up to 29.6 dB and 34.1 dB for the monopole and horn interferer antennas, respectively. This is mainly because of the short link length between the head and chest results in a relatively small path loss for this link, while at the same time the signal shadowing is also less severe than is the case for all the other paths contributing to the CIRs discussed here.

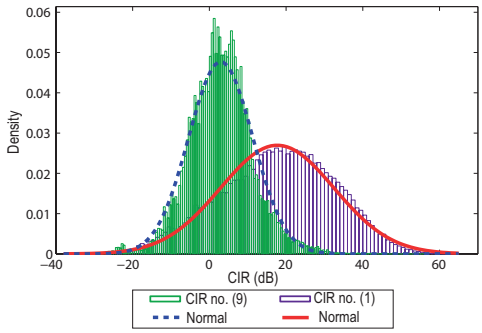

Fig. 13. Statistical distribution fitting of CIR no. (1) and (9).

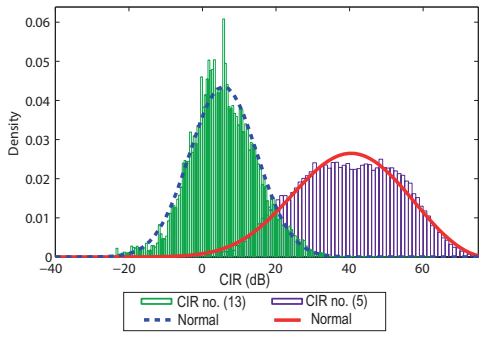

Fig. 14. Statistical distribution fitting of CIR no. (5) and (13).

Figs. 13 and 14 show the distribution fitting to the CIR histograms at 60 GHz and 2.45 GHz. The normal distribution fits are shown together with histograms of the measured CIR, expressed in dB. The NRMSE values were calculated for each distribution candidate and are shown in Tables IV and V, with their values being better than -0.42. Similarly to the P_I case, the CIR distribution fit is adequate due to the multi-modal and non-stationary nature of the CIR stochastic process. The parameters of the fitted statistical distributions for all CIRs are summarized in Tables IV and V.

V. Conclusion

An empirical study has been conducted to investigate interference between two persons wearing WBANs in an indoor environment at 60 GHz and 2.45 GHz. Both monopole and horn antennas were used and two subjects performed continuously random movements during the measurements.

This article has been accepted for publication in a future issue of this journal, but has not been fully edited. Content may change prior to final publication. Citation information: DOI 10.1109/TAP.2015.2465856, IEEE Transactions on Antennas and Propagation

TABLE IV
CIR STATISTICS (IN dB) FOR MEASURED ON-BODY CHANNELS AT 60 GHz

Scenario	CIR no.	CIR expression	$\widetilde{\text{CIR}}$	$\overline{\text{CIR}}$	σ_{CIR}	fit(Normal)
A	(1)	$(D^1_{Head,H}, S^1_{Abdomen,M}, S^2_{Head,H})$	18.4	17.7	14.8	-0.41
	(2)	$(D^1_{Head,H}, S^1_{Abdomen,M}, S^2_{Abdomen,M})$	16.2	15.6	13.1	-0.41
B	(3)	$(D^1_{Abdomen,M}, S^1_{Head,H}, S^2_{Abdomen,M})$	10.1	9.9	13.4	-0.41
	(4)	$(D^1_{Abdomen,M}, S^1_{Head,H}, S^2_{Head,H})$	15.6	14.8	14.2	-0.42
C	(5)	$(D^1_{Head,H}, S^1_{Chest,M}, S^2_{Head,H})$	39.5	39.2	14.4	-0.41
	(6)	$(D^1_{Head,H}, S^1_{Chest,M}, S^2_{Chest,M})$	36.1	35.7	13.0	-0.42
D	(7)	$(D^1_{Chest,M}, S^1_{Head,H}, S^2_{Chest,M})$	28.2	26.6	14.3	-0.41
	(8)	$(D^1_{Chest,M}, S^1_{Head,H}, S^2_{Head,H})$	32.5	31.4	13.9	-0.41

TABLE V
CIR STATISTICS (IN dB) FOR MEASURED ON-BODY CHANNELS AT 2.45 GHz

Scenario	CIR no.	CIR expression	$\widetilde{\text{CIR}}$	$\overline{\text{CIR}}$	σ_{CIR}	fit(Normal)
A'	(9)	$(D^1_{Head}, S^1_{Abdomen}, S^2_{Head})$	2.9	2.96	8.36	-0.42
	(10)	$(D^1_{Head}, S^1_{Abdomen}, S^2_{Abdomen})$	5.8	5.49	9.18	-0.41
B'	(11)	$(D^1_{Abdomen}, S^1_{Head}, S^2_{Abdomen})$	-0.2	0.26	10.40	-0.41
	(12)	$(D^1_{Abdomen}, S^1_{Head}, S^2_{Head})$	2.0	1.85	10.50	-0.42
C'	(13)	$(D^1_{Head}, S^1_{Chest}, S^2_{Head})$	5.4	5.68	9.17	-0.41
	(14)	$(D^1_{Head}, S^1_{Chest}, S^2_{Chest})$	6.5	7.12	9.66	-0.41
D'	(15)	$(D^1_{Chest}, S^1_{Head}, S^2_{Chest})$	8.8	9.23	9.71	-0.41
	(16)	$(D^1_{Chest}, S^1_{Head}, S^2_{Head})$	8.6	8.85	9.00	-0.41

Multiple antenna placements on the body were investigated. By adopting a 60 GHz carrier frequency with monopole antennas, the median interference level was reduced up to 20 dB compared to 2.45 GHz. By using horn antennas at 60 GHz, a further 20 dB reduction of the median interference level was observed for the same WBAN-to-WBAN separation and orientation distributions. Hence, directional antennas can not only amplify the wanted on-body link signals but can also minimize potential interference. Moreover, it was observed that WBANs suffer higher levels of interference when placing an antenna on the wrist due to its highly mobile nature.

The instantaneous CIRs for multiple channels with different interferers were also investigated. Due to the limited number of antennas, a horn-monopole antenna pair at 60 GHz was placed on each subject. The CIR is generally determined by the type of antennas and the physical on-body link length in the wanted channel, type of antenna for the interferer and the positions at which the antennas are placed. The best median CIR of 39.5 dB was achieved for the head-chest channel with a horn antenna interferer on the second subject at 60 GHz and a WBAN-to-WBAN separation less than 2.5 m as measured by the position of the two persons in the rectangle of Fig. 7. The same measurements were repeated at 2.45 GHz with all antennas being monopoles on the both subjects, and best median CIR was 8.8 dB for the head-chest channel. It is expected that higher CIR can be achieved by using only directional antennas on both subjects at 60 GHz. The measured interference power and CIRs were fitted to the normal distribution with a NRMSE fit metric greater than -0.42.

Due to the limitations of measurement setup, only two subjects can be considered in this study and they can only perform random movements in a small fixed area. Based on this study, 60 GHz multi-hop WBANs with short individual on-body links are a promising solution for reliable and interference-resilient body-centric communications. As always, a trade-off needs to be made between system complexity and reliability, depending on different applications and the intended density of WBAN deployments.

ACKNOWLEDGMENT

The authors thank the UK Engineering and Physical Sciences Research Council (EPSRC) for funding this research activity, under Grant Reference EP/I010491/1.

REFERENCES

[1] P. Hall and Y. Hao, *Antennas and Propagation for Body-Centric Wireless Communications*, ser. Artech House antennas and propagation library. Artech House, 2012.

[2] L. Hanlen, D. Miniutti, D. Rodda, and B. Gilbert, "Interference in body area networks: Distance does not dominate," in *IEEE 20th International Symposium on Personal, Indoor and Mobile Radio Communications*, Tokyo, Japan, 2009.

[3] B. de Silva, A. Natarajan, and M. Motani, "Inter-user interference in body sensor networks: Preliminary investigation and an infrastructure-based solution," in *Sixth International Workshop on Wearable and Implantable Body Sensor Networks*, Berkeley, CA, USA, 2009.

[4] A. Yener, R. Yates, and S. Ulukus, "Interference management for CDMA systems through power control, multiuser detection, and beamforming," *IEEE Transactions on Communications*, vol. 49, no. 7, pp. 1227–1239, 2001.
[5] I. Khan, Y. Nechayev, K. Ghanem, and P. Hall, "BAN-BAN interference rejection with multiple antennas at the receiver," *IEEE Transactions on Antennas and Propagation*, vol. 58, no. 3, pp. 927–934, 2010.
[6] H. Xiong, W. Zhang, Z. Du, B. He, and D. Yuan, "Front-end narrowband interference mitigation for DS-UWB receiver," *IEEE Transactions on Wireless Communications*, vol. PP, no. 99, pp. 1–10, 2013.
[7] X. Cheng and Y. Guan, "Narrow-band interference suppression in impulse radio ultra-wideband systems," *IEEE Transactions on Vehicular Technology*, vol. PP, no. 99, pp. 1–1, 2013.
[8] Y. Wang, I. Bonev, J. Nielsen, I. Kovacs, and G. Pedersen, "Characterization of the indoor multiantenna body-to-body radio channel," *IEEE Transactions on Antennas and Propagation*, vol. 57, no. 4, pp. 972–979, 2009.
[9] S. Cotton and W. Scanlon, "Channel characterization for single- and multiple-antenna wearable systems used for indoor body-to-body communications," *IEEE Transactions on Antennas and Propagation*, vol. 57, no. 4, pp. 980–990, 2009.
[10] S. Cotton, A. McKernan, and W. Scanlon, "Received signal characteristics of outdoor body-to-body communications channels at 2.45 GHz," in *Loughborough Antennas and Propagation Conference (LAPC)*, Loughborough, UK, 2011.
[11] Y. Nechayev, Z. Hu, and P. Hall, "Fading of the transmission channel between two wireless body area networks in an office at 2.45 GHz and 5.8 GHz," in *Loughborough Antennas and Propagation Conference (LAPC)*, Loughborough, UK, 2010.
[12] R. Rosini and R. D'Errico, "Off-body channel modelling at 2.45 GHz for two different antennas," in *6th European Conference on Antennas and Propagation (EUCAP)*, Prague, Czech Republic, 2012.
[13] L. Hanlen, D. Miniutti, D. Smith, D. Rodda, and B. Gilbert, "Co-channel interference in body area networks with indoor measurements at 2.4 GHz: Distance-to-interferer is a poor estimate of received interference power," *International Journal of Wireless Information Networks*, vol. 17, no. 3-4, pp. 113–125, 2010.
[14] S. Heaney, W. Scanlon, E. Garcia-Palacios, S. Cotton, and A. McKernan, "Characterization of inter-body interference in context aware body area networking (CABAN)," in *IEEE GLOBECOM Workshops (GC Wkshps)*, Houston, TX, USA, 2011.
[15] S. Cotton, W. Scanlon, and P. Hall, "A simulated study of co-channel inter-BAN interference at 2.45 GHz and 60 GHz," in *European Wireless Technology Conference (EuWIT)*, Paris, France, 2010.
[16] A. Pellegrini, A. Brizzi, L. Zhang, K. Ali, Y. Hao, X. Wu, C. Constantinou, Y. Nechayev, P. Hall, N. Chahat, M. Zhadobov, and R. Sauleau, "Antennas and propagation for body-centric wireless communications at millimeter-wave frequencies: A review," *IEEE Antennas and Propagation Magazine*, vol. 55, no. 4, pp. 262–287, 2013.
[17] X. Wu, L. Akhoondzadeh-Asl, and P. Hall, "Printed YagiUda array for on-body communication channels at 60 GHz," *Microwave and Optical Technology Letters*, vol. 53, no. 12, pp. 2728–2730, 2011.
[18] N. Chahat, M. Zhadobov, S. Muhammad, L. L. Coq, and R. Sauleau, "60-GHz textile antenna array for body-centric communications," *IEEE Transactions on Antennas and Propagation*, vol. 61, no. 4, pp. 1816–1824, 2013.
[19] N. Chahat, M. Zhadobov, L. L. Coq, S. Alekseev, and R. Sauleau, "Characterization of the Interactions Between a 60-GHz Antenna and the Human Body in an Off-Body Scenario," *IEEE Transactions on Antennas and Propagation*, vol. 60, no. 12, pp. 5958–5965, 2012.
[20] N. Chahat, M. Zhadobov, L. L. Coq, and R. Sauleau, "Wearable endfire textile antenna for on-body communications at 60 GHz," *IEEE Antennas and Wireless Propagation Letters*, vol. 11, pp. 799–802, 2012.
[21] Y. Nechayev, X. Wu, C. Constantinou, and P. Hall, "Millimetre-wave path-loss variability between two body-mounted monopole antennas," *IET Microwaves, Antennas Propagation*, vol. 7, no. 1, pp. 1–7, 2013.
[22] C. Constantinou, Y. Nechayev, X. Wu, and P. Hall, "Body-area propagation at 60 GHz," in *Loughborough Antennas and Propagation Conference (LAPC)*, Loughborough, UK, 2012.
[23] X. Wu, Y. Nechayev, C. Constantinou, and P. Hall, "Investigation of inter-user interference of wireless body area networks at 60 GHz," in *IEEE Antennas and Propagation Society International Symposium (APSURSI)*, Chicago, IL, USA, 2012.
[24] X. Wu, Y. Nechayev, C. Constantinou, P. Hall, A. Brizzi, A. Pellegrini, Y. Hao, and C. Parini, "Preliminary estimate for observability of 60 GHz wireless body area networks," in *IEEE Asia-Pacific Conference on Antennas and Propagation (APCAP)*, singapore, 2012.
[25] S. Gabriel, R. Lau, and C. Gabriel, "The dielectric properties of biological tissues: Iii. parametric models for the dielectric spectrum of tissues," *Physics in medicine and biology*, vol. 41, no. 11, p. 2271, 1996.
[26] M. DeGroot and M. Schervish, *Probability and Statistics*. Addison-Wesley, 2012.
[27] P. Hall, Y. Hao, Y. Nechayev, A. Alomainy, C. Constantinou, C. Parini, M. Kamarudin, T. Salim, D. Hee, R. Dubrovka, A. Owadally, W. Song, A. Serra, P. Nepa, M. Gallo, and M. Bozzetti, "Antennas and propagation for on-body communication systems," *IEEE Antennas and Propagation Magazine*, vol. 49, no. 3, pp. 41–58, June 2007.

Xianyue Wu (M'11) received the B.Eng. degrees in automation and electronic electrical engineering (First Class) at Harbin Institute of Technology, China and the University of Birmingham, Edgbaston, U.K., respectively, in 2009. From 2009 to 2013, he was pursuing a PhD degree at the University of Birmingham, working on antenna design and channel characterization for wireless body area networks. From November 2012 to May 2013, he was a visiting scholar at Charles L. Brown Department of Electrical and Computer Engineering and UVA Center for Wireless Health at the University of Virginia, USA. From 2014 to 2015, he was a research associate working on 5G research at Heriot-Watt University in Edinburgh, UK. Currently, he is with Huawei Shanghai Research Institute. He is the recipient of the Best Student Paper Prize at 2010 Loughborough Antennas & Propagation Conference, Honorable Mention in the Second International URSI Student Prize Paper Competition at the XXX URSI General Assembly and Scientific Symposium of International Union of Radio Science and Engineering and Physical Sciences Research Council (EPSRC) Studentship (2010-2013).

Yuriy I. Nechayev (M'00) received the Diploma of Specialist in Physics (hons.) from the Kharkiv State University, Kharkiv, Ukraine, in 1996, and the Ph.D. degree in electronic and electrical engineering from the University of Birmingham, Edgbaston, U.K., in 2004. From 2003 to 2014, he was with the University of Birmingham as a Research Associate, and later a Research Fellow, working on the problems of onbody propagation channel. Currently, he is with Huawei Technologies in Moscow, Russia. He has coauthored two book chapters, an IEEE magazine article, and a large number of technical papers on radio propagation in urban environments and around human body. His research interests include radiowave propagation modeling and measurements, propagation in random media, wave scattering, antennas, and electromagnetics.

Costas C. Constantinou (M'97) received the B.Eng. (Hons) degree in Electronic and Communications Engineering and Ph.D. degree in Electronic and Electrical Engineering from the University of Birmingham, U.K., in 1987 and 1991, respectively. In 1989, he joined the Faculty of the School of Electronic, Electrical and Systems Engineering, University of Birmingham, and is now a Reader in Communications Engineering. He heads the antennas and applied electromagnetics laboratory in the wireless communications and remote sensing research group and is currently director of research for the School. He has been involved in the antennas and propagation research for body area communications led by Prof. Peter Hall since its inception in 2002 and was the principal investigator on the efforts to extend this research to the 60 GHz band. He has published over 130 learned publications. His research interests in communications span a broad range of topics that includes optics, electromagnetic theory, electromagnetic scattering and diffraction, electromagnetic measurement, radiowave propagation modeling, mobile radio, wireless networks, and future communications networks architectures.

Peter S. Hall (M'88-SM'93-F'01) received the Ph.D. degree in antenna measurements from Sheffield University, Sheffield, U.K., in 1973. He is an Emeritus Professor with the Department of Electronic, Electrical and Computer Engineering, University of Birmingham, Edgbaston, U.K., which he joined in 1994. After graduating in 1973, he spent 3 years with Marconi Space and Defence Systems, Stanmore, U.K., working largely on a European Communications satellite project. He then joined The Royal Military College of Science, Swindon, U.K., as a Senior Research Scientist, progressing to Reader in Electromagnetics. He has published five books, over 350 learned papers, and taken various patents. He has researched extensively in the areas of antennas, propagation, and antenna measurements. Professor Hall is a Fellow of the IET and a past IEEE Distinguished Lecturer. He is a past Chairman of the IEE Antennas and Propagation Professional Group and past coordinator for Premium Awards for IEE Proceedings on Microwave, Antennas and Propagation. He is a member of the IEEE AP-S Fellow Evaluation Committee. He chaired the 1997 IEE ICAP conference, was Vice Chair of EuCAP 2008, and has been associated with the organization of many other international conferences. He was Honorary Editor of IEE Proceedings Part H from 1991 to 1995 and is currently on the Editorial Board of Microwave and Optical Technology Letters. He is a past member of the Executive Board of the EC Antenna Network of Excellence. He received the LAPC IET James Roderick James Lifetime Achievement Award in 2009 and the EurAAP Award and the IEEE AP-S John Kraus Award in 2012. His publications have earned many awards, including the 1990 IEE Rayleigh Book Award for the Handbook of Microstrip Antennas.